New Insights into the Action of Gravitons in Spiral Galaxies

Firmin J. Oliveira

East Asian Observatory, James Clerk Maxwell Submillimetre Telescope, Hilo, USA
Email: firmjay@hotmail.com

Abstract

New details of the action of gravitons in spiral galaxies are described. The effect of the graviton energy loss is hypothesized to be coupled to the baryon mass in the galaxy. From this relation, it follows that the baryonic Tully-Fisher relation is applicable to not just the final velocity of the galaxy but also to the rotational velocity at each radial position. In addition, a quadratic equation for the baryonic mass distribution is derived from the equation of motion. These results are demonstrated by making fits to galaxy rotation curves using a mass to light ratio model as well as the quadratic model for the mass distribution.

Keywords

Gravitons, Gravitational Redshift, Graviton Coupling Coefficient, Spiral Galaxies, Mass to Light Ratio

1. Introduction

This paper relates to the findings of the dynamics of spiral galaxy rotation curves found in [1] and I will use the data provided by the SPARC data base [2] to which that study refers. This is a development of my earlier paper [3]. There I introduced the idea that if gravitons exist, and given that they are bosonic relativistic particles, like photons but of spin 2, then like photons traveling in a gravitational field, the gravitons would experience a gravitational redshift as they go from a lower negative potential near the source mass to a higher potential going toward an orbiting mass. This energy loss $\delta\xi$ due to the redshift is expressed by,

$$\delta\xi(r) = -\frac{GM_b(r)m}{r^2}\delta r, \tag{1}$$

where G is Newton's gravitational constant, $M_b(r)$ is the baryonic source

mass at r, m is the relativistic mass of the gravitons and δr is a small change in the position of the gravitons. Integrating Equation (1) from the origin of the system of masses to the position r of the gravitons and multiplying by a coupling coefficient $K_g(r)$ of the gravitons to the mass at position r yields the total energy loss $\Delta \Xi(r)$ given by,

$$\Delta \Xi(r) = K_g(r) \int_0^r \delta \xi(s) = K_g(r) \int_0^r -\frac{GM_b(s)m}{s^2} ds. \tag{2}$$

Adding $\Delta \Xi(r)$ from Equation (2) to the standard energy equation of motion of an object of mass m in a circular orbit in the galaxy yields,

$$\frac{1}{2}mv^2(r) - \frac{GM_b(r)m}{r} - K_g(r) \int_0^r \frac{GM_b(s)m}{s^2} ds = -\frac{GM_b(r)m}{2r}. \tag{3}$$

Moving all terms except $v^2(r)$ from the left hand side to the right hand side of Equation (3) and simplifying yields the expressions for the rotational velocity at the radial distance r from the galaxy center, given by,

$$v^2(r) = \frac{GM_b(r)}{r} + 2K_g(r) \int_0^r \frac{GM_b(s)}{s^2} ds, \tag{4}$$

Equation (4) is the new equation that I will use to approximate the rotation curves of spiral galaxies.

From Equation (4) define the *normalization* $A(r)$,

$$A(r) = \frac{r}{Gv^2(r)}\left(1 - \frac{2K_g(r)}{v^2(r)} \int_0^r \frac{GM_b(s)}{s^2} ds\right). \tag{5}$$

Then, multiplying Equation (5) by $v^4(r)$ and substituting for $v^2(r)$ from Equation (4) and simplifying yields the baryonic Tully-Fisher relation (BTFR) [1] at any radial distance r for a spiral galaxy, given by,

$$M_b(r) = A(r)v^4(r). \tag{6}$$

To the extent that the predicted velocity $v(r) \approx v_{obs}(r)$ for any r of the galaxy, the BTFR is extended to the entire observed rotational velocity and mass range of the galaxy.

In the next section we describe how $K_g(r)$ can be related to $M_b(r)$.

2. The Connection of the Coupling Coefficient K_g to the Mass M

In previous studies I determined the value of the graviton coupling coefficient $K_g(r)$ at each radial distance r by the difference of the predicted velocity $v(r)$ and the observed velocity $v_{obs}(r)$, using Equation (4), implying that there was no predictive ability to the theory. While researching this problem, I noticed that the shapes of the $K_g(r)$ function and the normalized mass $M_b(r)/M_{gal}$ function were similar, though the mass had to be scaled in order to resemble the shape and size of $K_g(r)$. What I found was that with a constant scale factor k_f, a hypothetical relationship between the coupling coefficient $K_g(r)$ of Equation (4) and the baryonic mass $M_b(r)$ of the galaxy at radial distance r, can

be expressed by,

$$K_g(r) = k_f \frac{M_b(r)}{M_{gal}}, \tag{7}$$

where M_{gal} is the total galaxy baryonic mass and k_f is a constant scale factor determined by the fitting process. By substituting for $K_g(r)$ from Equation (7) into Equation (4) while evolving the mass $M_b(r)$ by iterations of the mass to light ratios Υ_*, the agreement of the theoretical velocities $v(r)$ to the observed velocities $v_{obs}(r)$ improves steadily. Again, from Equations (4) and (7), we obtain an expression for the scale factor k_f solved at the final observed position $r = r_f$ and velocity $v(r) = v(r_f) = v_f$ of the rotation curve, expressed by,

$$k_f = \frac{(v(r_f))^2 - \frac{GM_b(r_f)}{r_f}}{2\frac{M_b(r_f)}{M_{gal}}\int_0^{r_f}\frac{GM_b(s)}{s^2}ds} = \frac{v_f^2 - \frac{GM_{gal}}{r_f}}{2\int_0^{r_f}\frac{GM_b(s)}{s^2}ds}, \tag{8}$$

where we used the fact that at $r = r_f$, $M_b(r_f) = M_{gal}$. The total galaxy mass M_{gal} is a free parameter. Usually, for the fits, we can get the galaxy total baryonic mass from the BTFR, where $M_{gal} = AV_f^x$, where $A = 50$ and $x = 4$ [1], where it is confirmed that the value for the normalization parameter, equation (5), at the final position r_f approaches the value $A(r_f) = 50$. Or we can estimate the total galaxy mass by other means. After the fit is made for the galaxy curve, then the question to be addressed is whether the values of the mass to light ratios for the disk and bulge, Υ_{dsk} and Υ_{bul} respectively, are in agreement with observation, for which the surface brightness determination will be used.

In the next section we make rough fits to some galaxies and show the similarity between the coupling coefficient $K_g(r)$ and the normalized galaxy mass.

3. Rough Fits to SPARC Galaxy Rotation Curves Using the Mass to Light Ratio Model

I will illustrate how rough fits are made to galaxy rotation curves using data from the SPARC data base [2]. The fitting parameters are the BTFR total galaxy mass M_{gal}, the scale factor k_f and the mass to light ratios for the disk Υ_{dsk} and bulge Υ_{bul}. As a demonstration, I have carried this through for spirals NGC 2403, NGC 2481, and for dwarf spiral NGC 6503. (I will make finer, more precise fits in the next section of the paper.)

In the case of the SPARC data, the mass $M_b(r)$ is given as a functional form up to the mass to light ratios for the Υ_*, which are determined by fitting to the observed galaxy rotation curve.

From the photometric 3.6 mm data which has been reduced to the equivalent velocities for the galaxy disk and bulge and, as well, for the HI/Hα gas mass content, the mass radial distribution within the radius r from the galaxy center is given by,

$$M_b(r) = \frac{r}{G}\left(|v_{gas}(r)|v_{gas}(r) + \Upsilon_{dsk}(r)|v_{dsk}(r)|v_{dsk}(r) + \Upsilon_{bul}(r)|v_{bul}(r)|v_{bul}(r)\right), \tag{9}$$

where $r = r_i$, $i = 1, 2, \cdots, N$, $N > 1$, N the number of radial distances observed, and the absolute values of the velocities are needed because they can sometimes be negative (Ref. [4], p. 5) . For the SPARC model the velocities for the disk and bulge from **Table 2** of [2] are assumed to be $\Upsilon_* = 1$.

In **Table 1** and **Table 2** are the results of the rough fits to the galaxies, where Υ_* for the disk and bulge are fixed to values which give a reasonable fit to galaxy rotation velocity and with a galaxy mass approximately as given by the BTFR. The graviton coefficient k_f is computed at the final observed position r_f and velocity v_f for the galaxy. Notice that the normalization A for the final data point is about 50 for each galaxy. It is quite straight forward to make these fits and the masses are determined automatically by this algorithm.

Figures 1-**3** give plots for the rough fits to the galaxy rotation curves, with the distribution for the coefficient $K_g(r)$, the BTFR normalization $A(r)$ and the rotation curve showing the full curve along with the Newtonian and graviton energy loss velocity components. Note the upper plots in the figures showing the resemblance of the traces for $K_g(r)$ and for the scaled and displaced mass ratio $M_b(r)/M_{gal}$. The resemblence is apparent especially in the outer radial portions which shows the traces mostly overlaid. This result is most apparent in the plots of the fine fits, where all traces are virtually completely overlaid.

4. Fine Fits to SPARC Galaxy Rotation Curves Using the Mass to Light Ratio Model

To refine the galaxy fits, the same procedure is followed as for the rough fits,

Table 1. Rough fit results to SPARC galaxy data using the graviton model Equation (4) with masses from the SPARC mass model. The estimated baryonic masses in columns 2 and 3 and the normalization A are computed at the last radial position of the curve.

Galaxy	M_b ($M_\odot \times 10^{10}$)	$^\dagger M_b$ BTFR ($M_\odot \times 10^{10}$)	A ($M_\odot \cdot s^4 \cdot km^{-4}$)
NGC 2403	1.653	1.612	51.275
NGC 2841	24.017	37.356	49.393
NGC 6503	1.109	0.875	51.459

†Using the final velocity as the flat velocity.

Table 2. Rough fit results to SPARC galaxy data using the graviton model Equation (4). The columns for Υ_{dsk} and Υ_{bul} are the fixed values used in the fits. Zero (0) in the Υ_{bul} column means the bulge velocity is zero in the data. The MAE is the average absolute error for each fit.

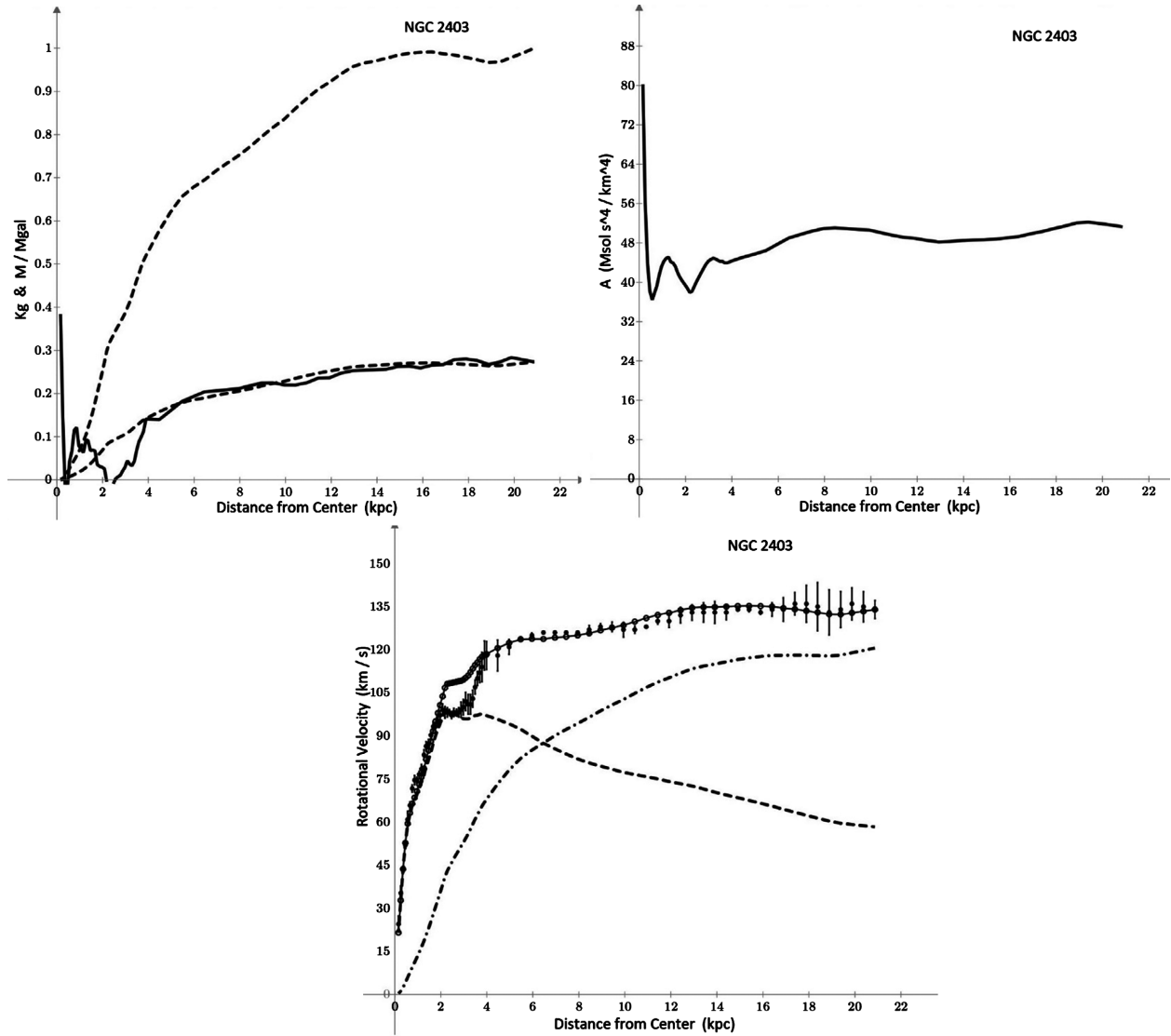| Galaxy	Υ_{dsk} ($M_\odot L_\odot^{-1}$)	Υ_{bul} ($M_\odot L_\odot^{-1}$)	k_f	MAE (km·s^{-1})
NGC 2403	0.860	0	0.273	3.697
NGC 2841	1.164	1.043	0.205	5.717
NGC 6503	0.580	0	0.255	4.227

Figure 1. Rough fit made to NGC 2403 with SPARC data with velocity profiles for gas, disk and bulge. The top plot shows the unscaled normalized mass $M_b(r)/M_{gal}$ (dashed line), and the scaled and offset normalized mass (dashed line) along with the graviton coefficient K_g. The middle plot shows the normalization $A(r)$ parameter as a solid line. The bottom plot shows the rotation velocity $v(r)$ (solid line) with open circles, the data points (solid circles with error bars.) The dashed line is the velocity due to Newtonian theory, $GM_b(r)/r$. The dash-dot line is the velocity due to the graviton energy loss, given by the second term on the right hand side of Equation (4).

except that the mass to light ratios for the disk and bulge are varied by iterations at each radial position to minimize the error between the observed and theoretical velocities. The algorithm to iterate a new mass to light ratio is given by,

$$\Upsilon_*(r) \leftarrow \Upsilon_*(r)\frac{v_{obs}(r)}{v(r)}, \tag{10}$$

where a new velocity is determined by (4) using the newly iterated $\Upsilon_*(r)$, until the average velocity error MAE falls below a threshold value.

Looking at **Table 3** and **Table 4**, we see the fine fit results for each galaxy. The
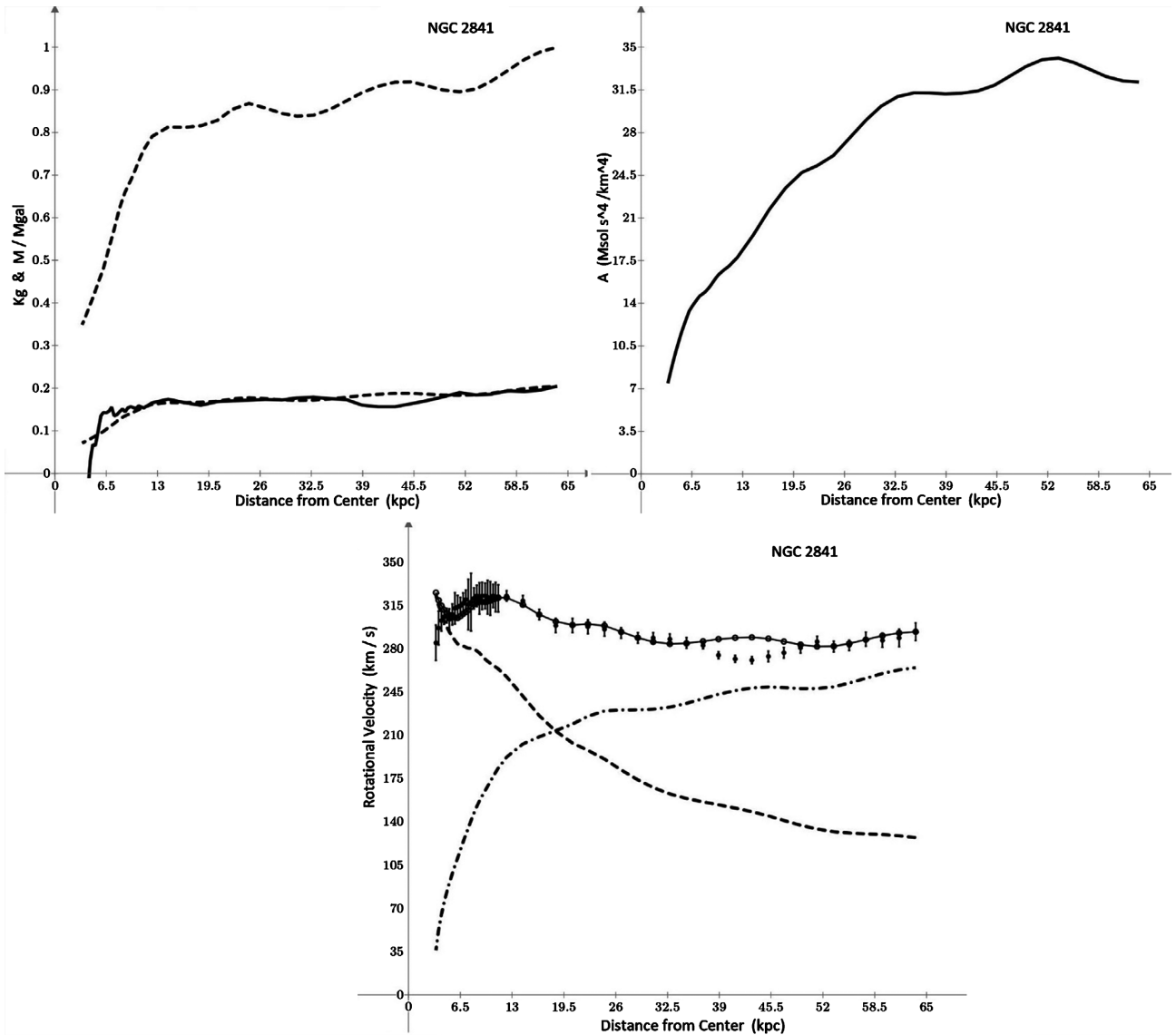
Figure 2. Rough fit made to NGC 2841 with SPARC data with velocity profiles for gas, disk and bulge. The top plot shows the unscaled normalized mass $M_b(r)/M_{gal}$ (dashed line), and the scaled and offset normalized mass (dashed line) along with the graviton coefficient K_g. The middle plot shows the normalization A parameter as a solid line. The bottom plot shows the rotation velocity (solid line) with open circles, the data points (solid circles with error bars). The dashed line is the velocity due to Newtonian theory, $GM_b(r)/r$. The dash-dot line is the velocity due to the graviton energy loss, given by the second term on the right hand side of Equation (4).

masses obtained are in good agreement with the BTFR masses, where the fitted mass is derived automatically as a result of making a good fit to the velocity curve, with the velocity *mean absolute error*[1] of $\text{MAE} < 1\,\text{km}\cdot\text{s}^{-1}$. The algorithm is simple and robust.

Figures 4-6 give plots for the fine fits to the galaxy rotation curves, with the distribution for the coefficient $K_g(r)$, the BTFR normalization $A(r)$, and the

---

[1]The mean absolute error is defined by $\text{MAE} = (1/n)\sum_{j=1}^{n}\|O_j - P_j\|$, where O_j are the observation values and P_j are the model predictor values.
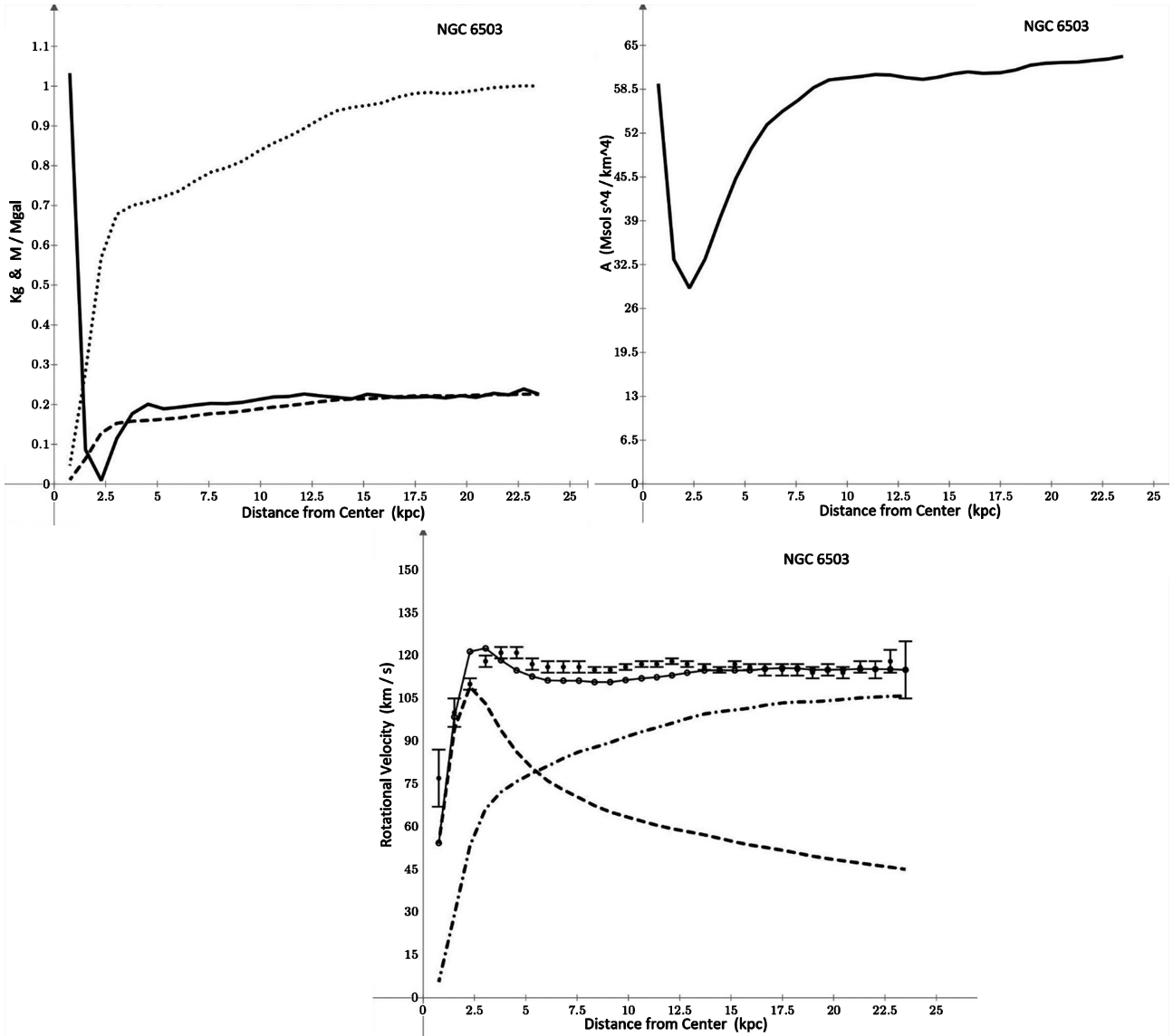
Figure 3. Rough fit made to NGC 6503 with SPARC data with velocity profiles for gas, disk and bulge. The top plot shows the unscaled normalized mass $M_b(r)/M_{gal}$ (dashed line), and the scaled and offset normalized mass (dashed line) along with the graviton coefficient K_g. The middle plot shows the normalization A parameter as a solid line. The bottom plot shows the rotation velocity (solid line) with open circles, the data points (solid circles with error bars). The dashed line is the velocity due to Newtonian theory, $GM_b(r)/r$. The dash-dot line is the velocity due to the graviton energy loss, given by the second term on the right hand side of Equation (4).

Table 3. Fine fit results to SPARC galaxy data using the graviton model (4) with masses from the SPARC mass model.

Galaxy	M_b ($M_\odot \times 10^{10}$)	$^\dagger M_b$ BTFR ($M_\odot \times 10^{10}$)	A ($M_\odot \cdot s^4 \cdot km^{-4}$)
NGC 2403	1.629	1.612	50.52
NGC 2841	37.353	37.356	49.996
NGC 6503	0.8524	0.8745	48.737
UGC A442	0.05095	0.05095	50

†Using the final velocity as the flat velocity.

Table 4. Fine fit results to SPARC galaxy data using the graviton model Equation (4). The columns for $\langle \Upsilon_{dsk} \rangle$ and $\langle \Upsilon_{bul} \rangle$ are average values obtained in the fits. Zero (0) in the Υ_{bul} column means the bulge velocity is zero in the data. The MAE is the average absolute error for each fit. For UGC A442, M_b, A and $\langle \Upsilon_{dsk} \rangle$ are determined by the mass to light fitting method, whilst the scale factor k_f and fitting error MAE are the results of the quadratic fitting method.

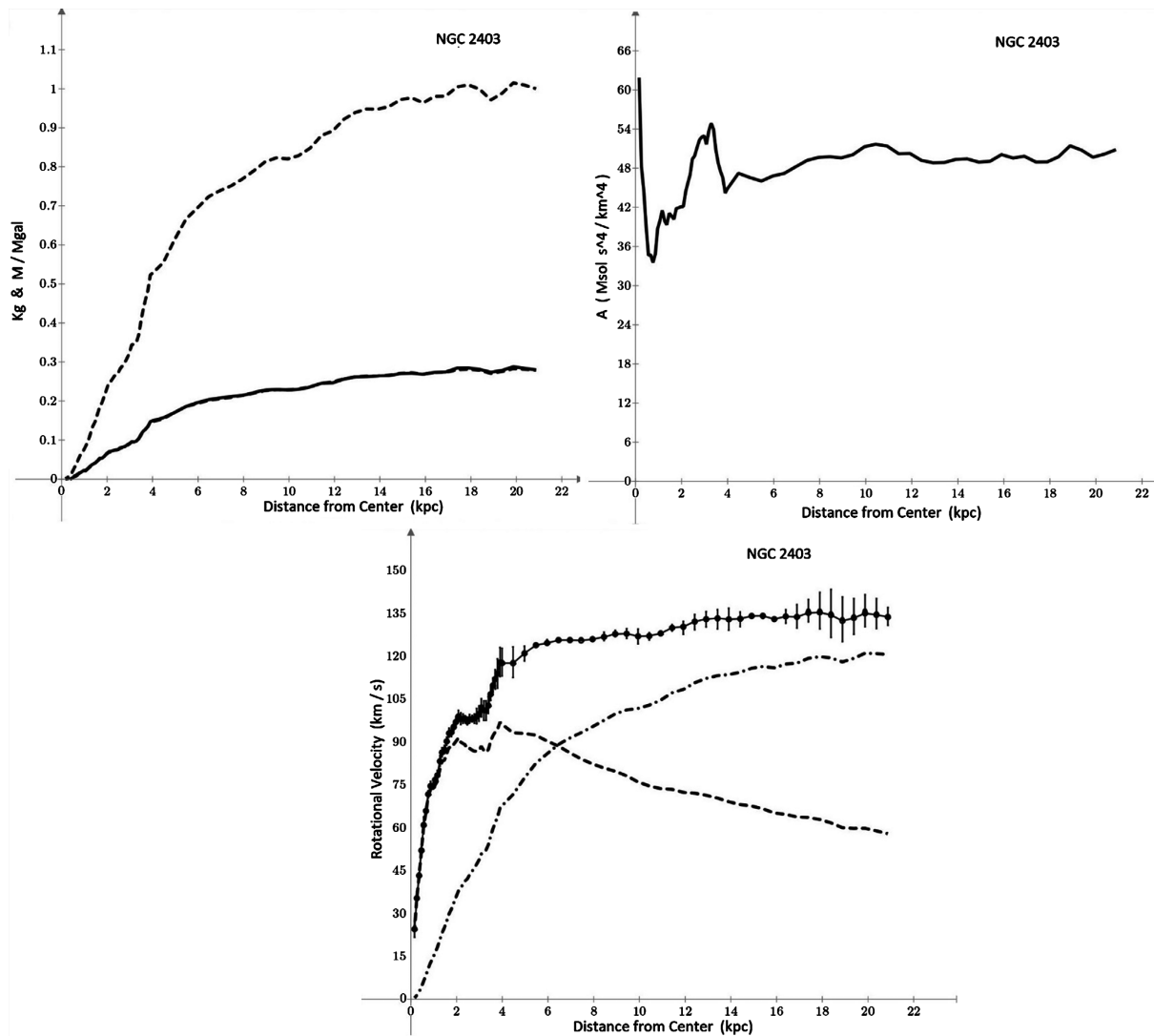| Galaxy	$\langle \Upsilon_{dsk} \rangle$ ($M_\odot L_\odot^{-1}$)	$\langle \Upsilon_{bul} \rangle$ ($M_\odot L_\odot^{-1}$)	k_f	MAE (km·s⁻¹)
NGC 2403	0.830	0	0.280	0.180
NGC 2841	1.101	1.485	0.155	0.351
NGC 6503	0.474	0	0.244	0.102
UGC A442	1.758	0	0.924	0.090

Figure 4. Fine fit made to NGC 2403 with SPARC data with velocity profiles for gas, disk and bulge. The top plot shows the unscaled normalized mass $M_b(r)/M_{gal}$ (dashed line), and the scaled and offset normalized mass (dashed line) along with the graviton coefficient K_g. The middle plot shows the normalization A parameter as a solid line. The bottom plot shows the rotation velocity (solid line) with open circles, the data points (solid circles with error bars). The dashed line is the velocity due to Newtonian theory, $GM_b(r)/r$. The dash-dot line is the velocity due to the graviton energy loss, given by the second term on the right hand side of Equation (4).
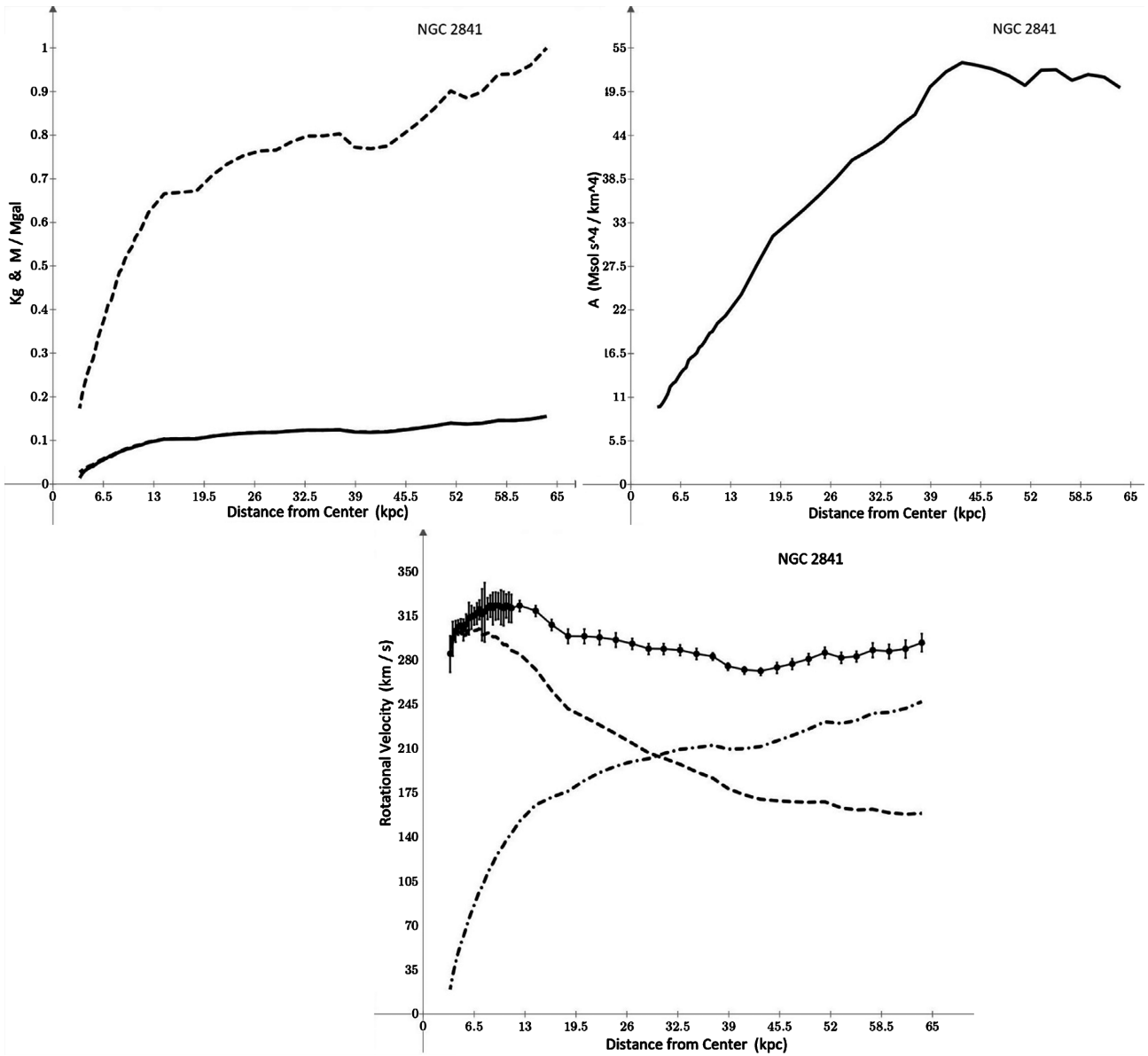
Figure 5. Fine fit made to NGC 2841 with SPARC data with velocity profiles for gas, disk and bulge. The top plot shows the unscaled normalized mass $M_b(r)/M_{gal}$ (dashed line), and the scaled and offset normalized mass (dashed line) along with the graviton coefficient K_g. The middle plot shows the normalization A parameter as a solid line. The bottom plot shows the rotation velocity (solid line) with open circles, the data points (solid circles with error bars). The dashed line is the velocity due to Newtonian theory, $GM_b(r)/r$. The dash-dot line is the velocity due to the graviton energy loss, given by the second term on the right hand side of Equation (4).

rotation curve showing the full curve along with the Newtonian and the graviton energy loss components.

5. Quadratic Equation for the Mass

A quadratic equation for the mass $M_b(r)$ is readily obtained from Equation (4). The second term on the right hand side of that equation can be split into two parts as follows,
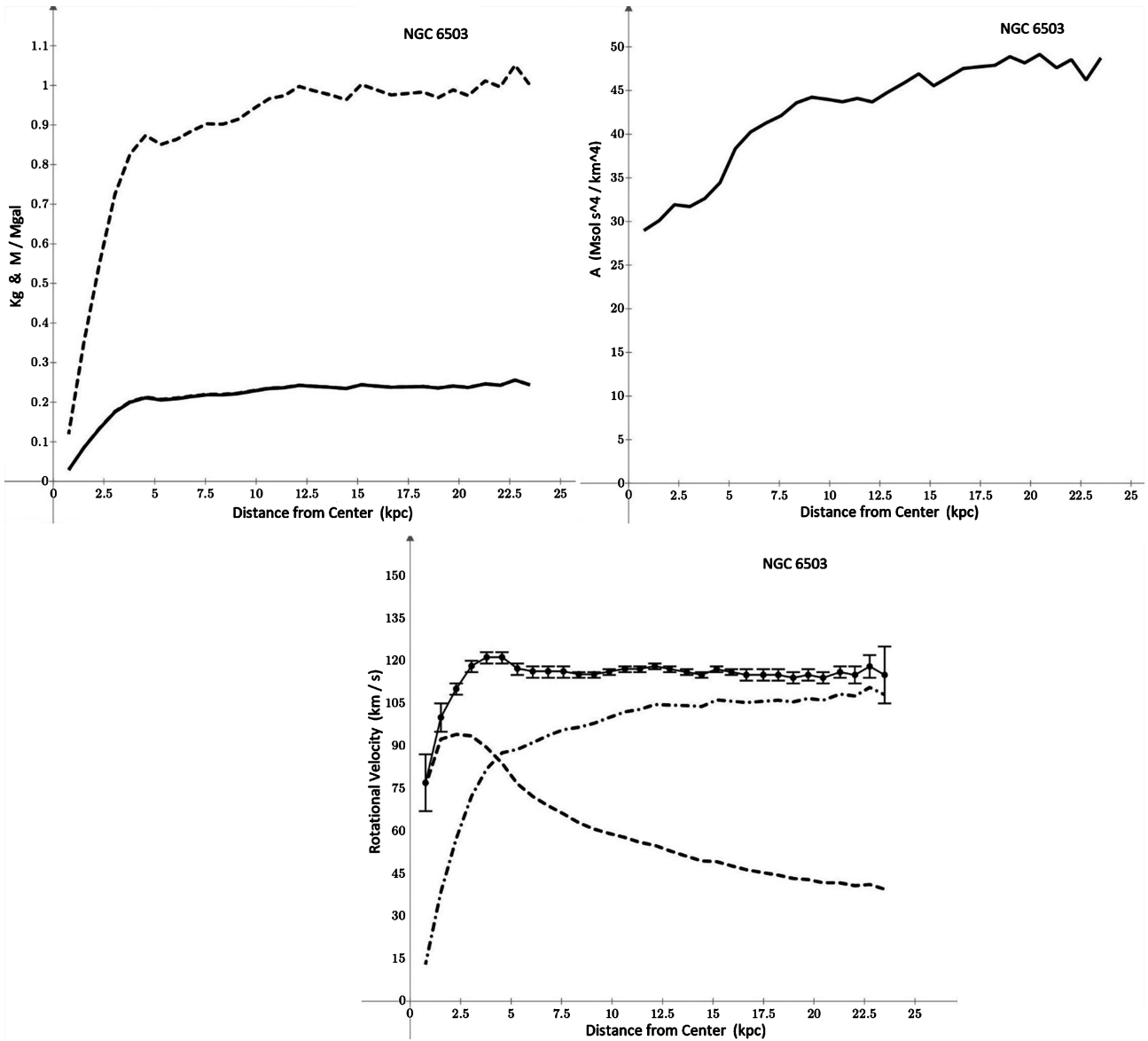
Figure 6. Fine fit made to NGC 6503 with SPARC data using velocity profiles for gas, disk and bulge. The top plot shows the unscaled normalized mass $M_b(r)/M_{gal}$ (dashed line), and the scaled and offset normalized mass (dashed line) along with the graviton coefficient K_g. The middle plot shows the normalization A parameter as a solid line. The bottom plot shows the rotation velocity (solid line) with open circles, the data points (solid circles with error bars). The dashed line is the velocity due to Newtonian theory, $GM_b(r)/r$. The dash-dot line is the velocity due to the graviton energy loss, given by the second term on the right hand side of Equation (4).

$$2K_g(r)\int_0^r \frac{GM_b(s)}{s^2}\,\mathrm{d}s = 2K_g(r)\int_0^{r_i} \frac{GM_b(s)}{s^2}\,\mathrm{d}s + 2K_g(r)\int_{r_i}^r \frac{GM_b(s)}{s^2}\,\mathrm{d}s, \quad (11)$$

where $r_i < r$ and in the second term on the right hand side, in the integrand, it is assumed that $M_b(s) \approx M_b(r)$ for $r_i \leq s \leq r$. In other words, for a small enough interval $\Delta r = r - r_i$, the galaxy mass at that interval is the mass at radial position r. Thus in the above Equation (11), in the second term on the right hand side, the mass in the integrand can be moved out of the integral, giving,

$$2K_g\left(r\right)\int_{r_i}^{r}\frac{GM_b\left(s\right)}{s^2}\mathrm{d}s = 2K_g\left(r\right)M_b\left(r\right)\int_{r_i}^{r}\frac{G}{s^2}\mathrm{d}s = 2k_f\frac{\left(M_b\left(r\right)\right)^2}{M_{gal}}\int_{r_i}^{r}\frac{G}{s^2}\mathrm{d}s, \quad (12)$$

since, from Equation (7), $K_g\left(r\right) = k_f M_b\left(r\right)/M_{gall}$, we observe that this term of Equation (12) has the square of the mass, $\left(M_b\left(r\right)\right)^2$.

Combining the results of Equations (11) and (12) into Equation (7), after some manipulations, yields the equation quadratic in $M_b\left(r\right)$,

$$\left(\frac{2k_f G}{M_{gal}}\int_{r_i}^{r}\frac{\mathrm{d}s}{s^2}\right)\left(M_b\left(r\right)\right)^2 + \left(\frac{G}{r}+\frac{2k_f G}{M_{gal}}\int_{0}^{r_i}\frac{GM_b\left(s\right)}{s^2}\mathrm{d}s\right)M_b\left(r\right) - \left(v\left(r\right)\right)^2 = 0. \quad (13)$$

By defining the three parameters $a\left(r\right)$, $b\left(r\right)$ and $c\left(r\right)$ in the form,

$$a\left(r\right) = \frac{2k_f G}{M_{gal}}\int_{r_i}^{r}\frac{\mathrm{d}s}{s^2}, \quad (14)$$

$$b\left(r\right) = \frac{G}{r}+\frac{2k_f G}{M_{gal}}\int_{0}^{r_i}\frac{GM_b\left(s\right)}{s^2}\mathrm{d}s, \quad (15)$$

$$c\left(r\right) = -\left(v\left(r\right)\right)^2, \quad (16)$$

We obtain solutions for $M_b\left(r\right)$ in the familiar form,

$$M_b\left(r\right) = \frac{1}{2a\left(r\right)}\left(-b\left(r\right)+\sqrt{\left(b\left(r\right)\right)^2 - 4a\left(r\right)c\left(r\right)}\right), \quad (17)$$

where the positive square root was chosen to keep the mass positive and it is apparent that the quantity under the square root is always non-negative since $a\left(r\right)$ is positive and $c\left(r\right)$ is negative.

6. Fits to SPARC Galaxy Rotation Curves Using the Quadratic Solution Mass Model

The remarkable thing is that by using the observed velocity $v_{obs}\left(r\right)$ for $v\left(r\right)$ in Equation (16) we obtain estimations for the galaxy mass distribution directly from Equation (17). And then this mass estimation can be substituted into the velocity Equation (7) to obtain a predicted galaxy rotation velocity $v\left(r\right)$. It is found that, with a galaxy total mass M_{gal} given by the BTFR, a fit with MAE error < 0.1 km·s⁻¹ is obtained for the entire rotation curve by, most often, just three iterations.

Table 3 and Table 4 give the fitting results for UGC A442 [5] using a combination of the mass to light ratio fitting method and the quadratic fitting method.

Figure 7 shows plots for data from spiral galaxy UGC A442. The upper plot is of the normalization parameter $A\left(r\right)$ from Equation (5) obtained with the mass distribution from the quadratic Equation (17). The middle plot shows the fit to the rotation velocity curve using the mass from the quadratic fit substituted into Equation (4). The lower plot is a comparison of the mass obtained from the mass to light ratio fit (method used in the above galaxy analyses) and the mass determined by the quadratic fit.
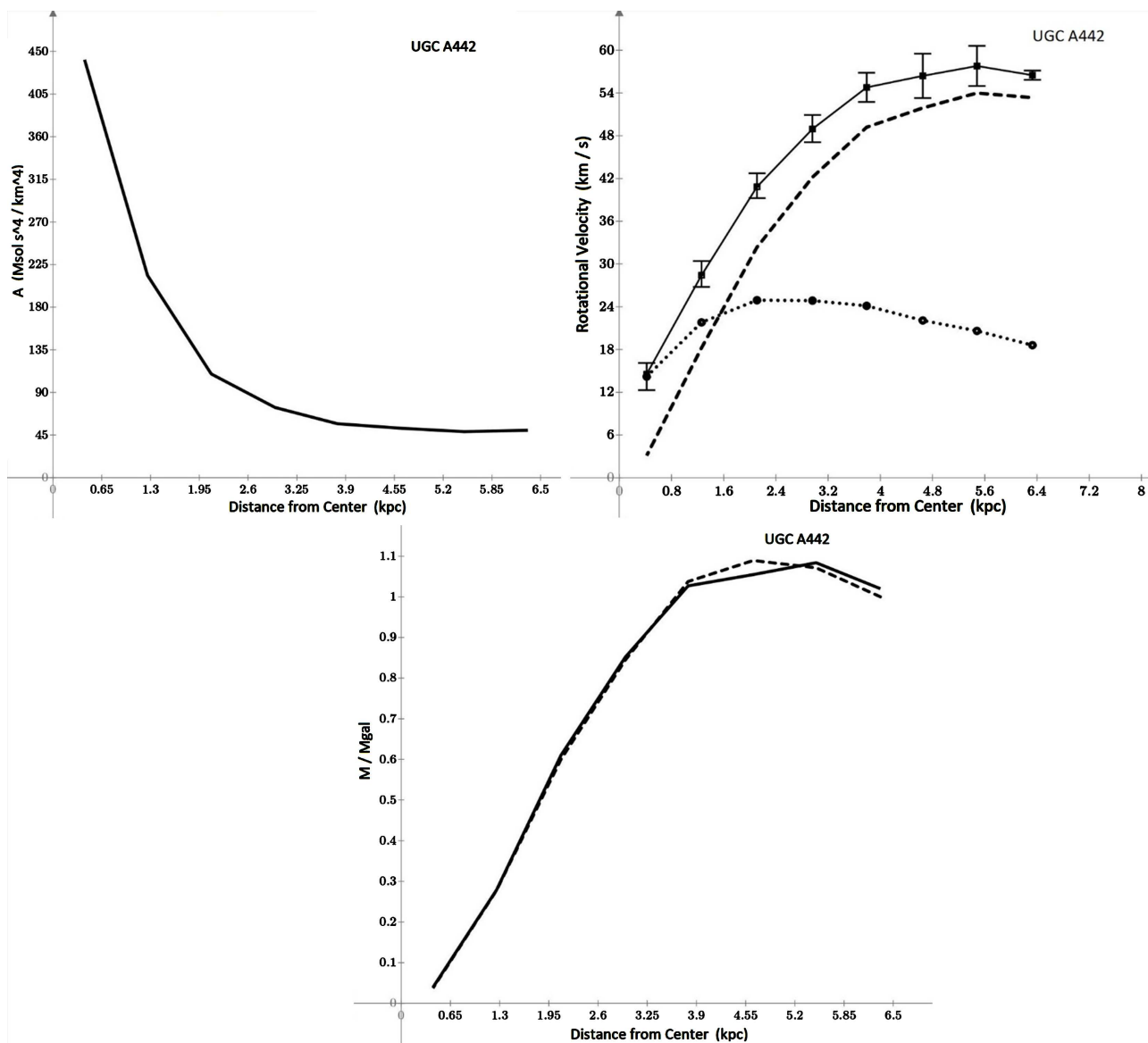
Figure 7. Galaxy UGC A442 from SPARC data. The upper plot is the normalization parameter $A(r)$. The middle plot is the rotation velocity $v(r)$ (solid line) along with the Newtonian velocity curve (dotted line with open circles) and the graviton energy loss velocity contribution (dashed line). The bottom plot shows the comparison of the normalized mass (M/M_{gal}), obtained from the mass to light fitting method (dashed line) and from the quadratic fitting method (solid line).

7. Discussion

This limited study provides evidence of the proportionality of the coupling coefficient $K_g(r)$ at each radial position to the normalized baryon mass $M_b(r)/M_{gal}$ at that position. The fitting algorithm has a single constraint to satisfy: fitting to all the observed rotation velocities. A judgement for the quality of the fit is that the total galaxy mass should be compatible with the mass determined by the BTFR for the galaxy, with small total average error for the rotation velocities , and that the mass to light ratios distribution, as well as the surface brightnesses, should correspond to that determined by photometric observations.

Comparing the total derived galaxy masses in the fine fits to the stellar plus gas masses reported in (Ref. [2], **Table 1**) we have, in units of $10^{10}\,\mathrm{M}_\odot$, for NGC 2403 the derived mass is $M_{b2403} = 1.629$ compared to stellar and gas mass of $1.1 + 0.47 = 1.57$, implying that the derived total galaxy mass is 4% greater than [2]. For NGC 2841 the derived mass is $M_{b2841} = 38.443$ compared to stellar and gas mass of $32.3 + 1.7 = 34.0$, meaning that the derived total mass is 10% larger. For NGC 6503, the derived mass is $M_{b6503} = 0.8524$, compared to the stellar and gas mass of $0.83 + 0.24 = 1.07$, so that the derived total mass is 20% smaller.

Figure 8 gives plots of the mass to light ratios from the fine fit procedure for the galaxies. **Table 4** gives the average values for the disk and bulge mass to light ratios obtained from the fits. The estimation formula for the disk mass to light ratio is 3/4 of the maximum disk mass to light ratio (Ref. [2], Υ_{max} for each galaxy is in col. 8 of **Table 1**). The average disk mass to light ratio (in units of $(\mathrm{M}_\odot \mathrm{L}_\odot^{-1})$ is $\Upsilon_* = 0.830$ for NGC 2403 compared to the formula estimate of
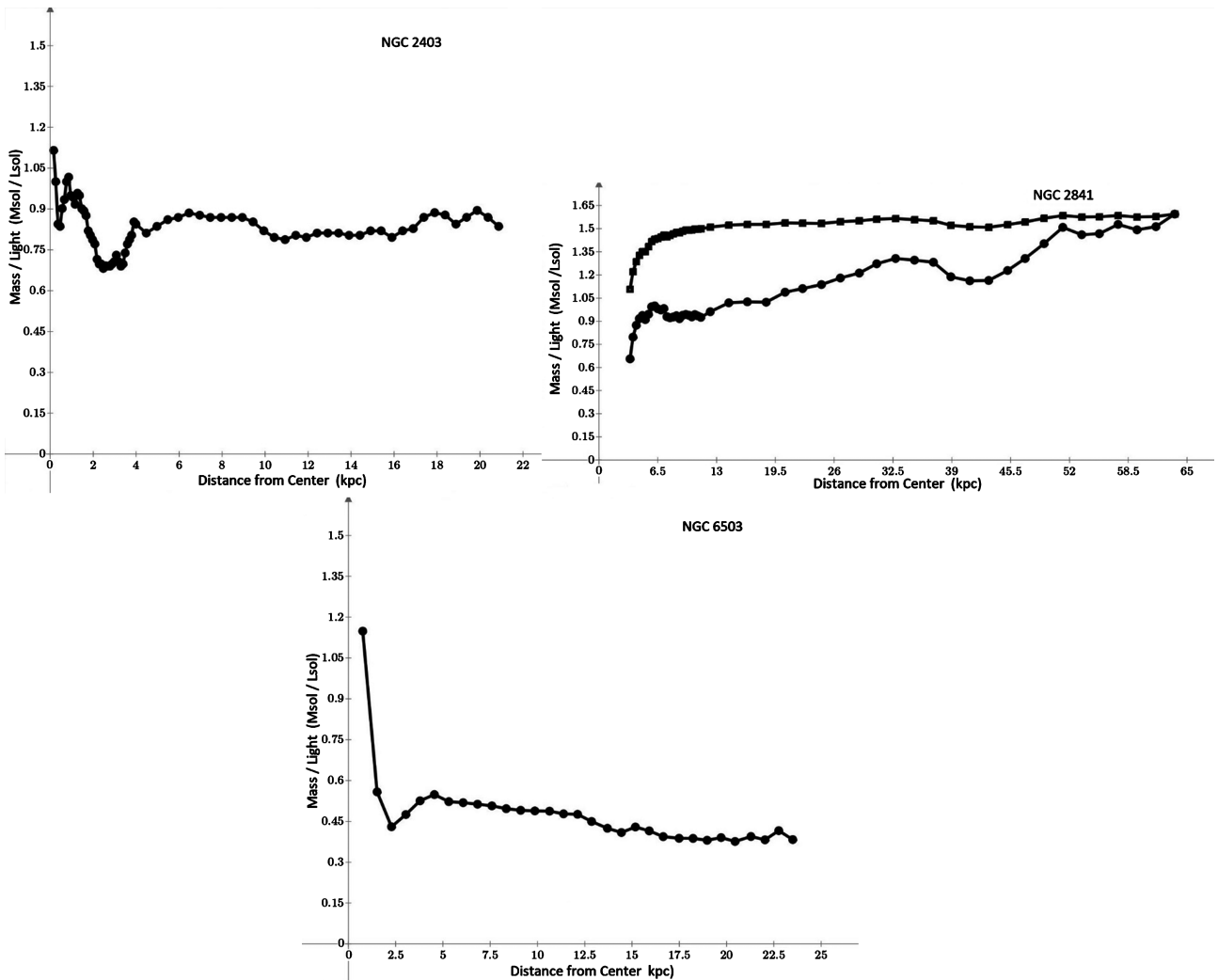

Figure 8. Mass to light ratios radial distribution (*M/L*) for fine fits made to NGC 2403, NGC 2841 and NGC 6503 with SPARC data. The distribution for the disk $\Upsilon_*(r)$ is the solid line with filled circles and for the bulge it is the solid line with + symbols. Only NGC 2841 has a bulge *M/L*.

$0.75 \times 1.5 = 1.1$. The average $\Upsilon_* = 2.5$ for NGC 2841 compared to the estimate of $0.75 \times 7.9 = 5.9$. The average $\Upsilon_* = 0.474$ for NGC 6503 compared to the estimate of $0.75 \times 1.7 = 1.3$.

Figure 9 gives plots of the surface brightness magnitudes for the fine fits to the galaxies. The surface brightness magnitudes are obtained from the mass to light ratios Υ_* and the mass distribution $M_b(r)$ from the fits at each radial location of the data. Examining Equation (9), we see that the mass to light ratio Υ_* is dimensionless, so that the luminosity $L(r)$ at radial position r of the galaxy, which is usually specified in Janskys = Watts/m²/Hz, is equivalent to a surface mass density related to the mass $M_b(r)$ and the mass to light ratio $\Upsilon_*(r)$ expressed by,

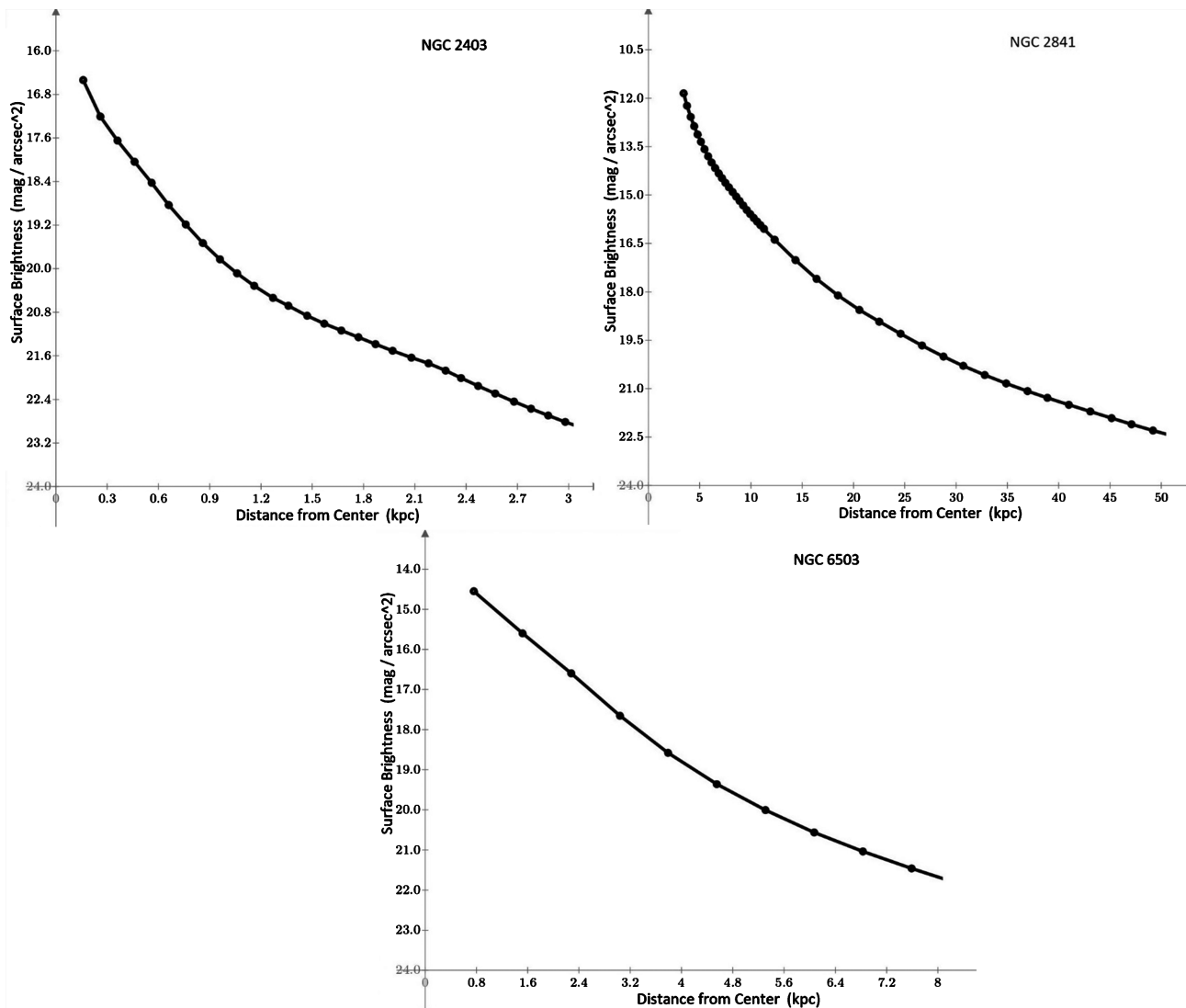$$L(r) = \frac{1}{4\pi r^2} \frac{M_b(r)}{\Upsilon_*(r)}. \tag{18}$$

Figure 9. Surface brightness magnitudes for fine fits made to NGC 2403, NGC 2841 and NGC 6503 with SPARC data made using Equation (19).
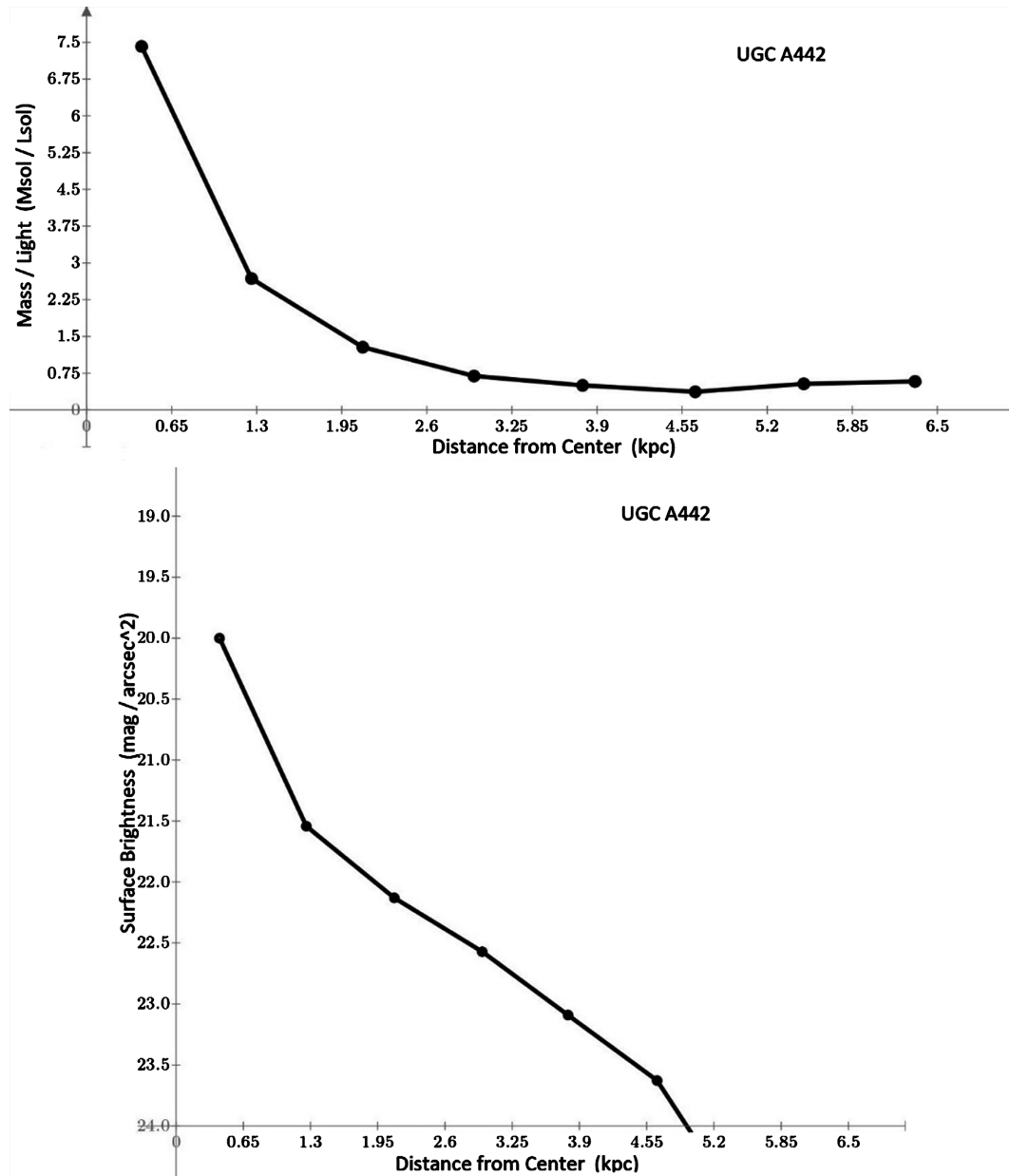
Figure 10. Galaxy UGC A442 from SPARC data. Mass to light ratio (upper plot) and surface brightness (lower plot) using Equation (19) with Υ_* from the mass to light ratio fit and the mass from the quadratic fit to the galaxy rotation curve.

Using Equation (18), the surface brightness $\mu(r)$ in the logrithmic scale of magnitudes per square radian is given by,

$$\mu(r) - \mu_0 = -2.5\log\left(\frac{L(r)}{(r/d)^2}\right) = -2.5\log\left(\frac{d^2}{4\pi r^4}\frac{M_b(r)}{\Upsilon_*(r)}\right), \qquad (19)$$

where d is the distance to the galaxy and μ_0 is a reference brightness. The surface brightness, Equation (19), is typically converted to magnitude per square arcsecond. For NGC 2403, the magnitude range for the fit is 16.5 at 0.16 kpc and drops to 24.5 at 5 kpc compared to the observed variation [5] of about 16.5 mag

arcsec^{-2} at 0 kpc to 21 mag. at 5 kpc, which is a poor agreement. For NGC 2841, the magnitude range for the fit is 12.1 at 3.4 kpc to 19.3 at 24.6 kpc compared to the observed magnitude range of about 12.5 at 0 kpc to 22.5 at 24 kpc, which is also poorly matched. For NGC 6503 the magnitude range for the fit is 14.6 at 0.8 kpc to 22.2 at 9.9 kpc compared to the observed magnitude range of about 14.5 at 0 kpc to 23 at 10 kpc, a good match. The zero point references I used to approximately match the central galaxy magnitudes are $\mu_0 = 9.5$ for NGC 2403, $\mu_0 = 4.2$ for NGC 2841, and $\mu_0 = 5.8$ for NGC 6503. One major reason for the disagreements between my surface brightness results and the observed brightnesses is the lack of accounting for extinction of the signal in the interstellar medium, which will need to be addressed in future.

Figure 10 shows plots from galaxy UGC A442. The upper plot shows the mass to light ratio Υ_* determined by the mass to light fitting method. The lower plot shows the surface brightness magnitude for the galaxy using Equation (19). The derived surface brightness magnitude is 20 mag·arcsec^{-2} at the galaxy origin and about 24 at 5 kpc radial distance, which agrees quite well with the SPARC photometric result [5]. The zero point reference I used to approximately match the SPARC central galaxy magnitude is $\mu_0 = 7$ in Equation (19).

8. Conclusion

The theory of graviton gravitational redshift is physically sound and there is a minimum of arbitrariness, essentially only in the estimation of the coupling scale factor k_f expressed by Equation (8). Overall, the results of the theory and algorithms are quite remarkable. We will continue to access the SPARC galaxies database to verify the resiliency of this theory.

Conflicts of Interest

The author declares no conflicts of interest regarding the publication of this paper.

References

[1] McGaugh, S.S. (2005) The Baryonic Tully-Fisher Relation of Galaxies with Extended Rotation Curves and the Stellar Mass of Rotating Galaxies. *The Astrophysical Journal*, **632**, 859-871. https://doi.org/10.1086/432968

[2] SPARC (2020) http://astroweb.cwru.edu/SPARC/

[3] Oliveira, F.J. (2022) How the Redshift of Gravitons Explains Dark Matter and Dark Energy. *Journal of Modern Physics*, **13**, 1348-1368. https://doi.org/10.4236/jmp.2022.1311084

[4] Lelli, F., McGaugh, S.S. and Schombert, J.M. (2016) SPARC: Mass Models for 175 Disk Galaxies with Spitzer Photometry and Accurate Rotation Curves. *The Astrophysical Journal*, **152**, 157-170. https://doi.org/10.3847/0004-6256/152/6/157

[5] Chae, K., Lelli, F., Desmond, H., McGaugh, S.S., Li, P. and Schombert, J.M. (2020) Testing the Strong Equivalence Principle: Detection of the External Field Effect in Rotationally Supported Galaxies. *The Astrophysical Journal*, **904**, 51-70. https://doi.org/10.3847/1538-4357/abbb96